REPORT DOCUMENTATION PAGE

Public Reporting burden for this collection of information is estimated to average 1 hour per response, including the time for reviewing instructions, searching existing data sources, gathering and maintaining the data needed, and completing and reviewing the collection of information. Send comment regarding this burden estimates or any other aspect of this collection of information, including suggestions for reducing this burden, to Washington Headquarters Services, Directorate for information Operations and Reports, 1215 Jefferson Davis Highway, Suite 1204, Arlington, VA 22202-4302, and to the Office of Management and Budget, Paperwork Reduction Project (0704-0188,) Washington, DC 20503.

1. AGENCY USE ONLY (Leave Blank)	2. REPORT DATE 13 Aug 2009	3. REPORT TYPE AND DATES COVERED Final report 01 Sep 08-01 Jun 09

4. TITLE AND SUBTITLE
Novel Electro-analytical Tools for Phase-Transformation Electrode Materials

5. FUNDING NUMBERS

G--W911NF0810441

6. AUTHOR(S)
Chunsheng Wang and Yujie Zhu

7. PERFORMING ORGANIZATION NAME(S) AND ADDRESS(ES)
Department of Chemical and Biomolecular Engineering
University of Maryland, College Park
College Park, Maryland 20740

8. PERFORMING ORGANIZATION REPORT NUMBER

9. SPONSORING / MONITORING AGENCY NAME(S) AND ADDRESS(ES)
U. S. Army Research Office
P.O. Box 12211
Research Triangle Park, NC 27709-2211

10. SPONSORING / MONITORING AGENCY REPORT NUMBER

11. SUPPLEMENTARY NOTES The views, opinions and/or findings contained in this report are those of the author(s) and should not be construed as an official Department of the Army position, policy or decision, unless so designated by other documentation.

12 a. DISTRIBUTION / AVAILABILITY STATEMENT
Approved for public release; distribution unlimited.

12 b. DISTRIBUTION CODE

13. ABSTRACT (Maximum 200 words)

We measured and compared phase transformation accommodation energy (AE) for $Li_4Ti_5O_{12}$ and $LiFePO_4$ with different particle size by using of galvanostatic intermittent titration (GITT). The results showed that charge AE was larger than that for discharge; The AE for the 1st cycle was larger than next cycles due to inducing of defects; Because of smaller volume difference, AE of $Li_4Ti_5O_{12}$ was lower than that of $LiFePO_4$; AE of $LiFePO_4$ with small particle size was lower than that of $LiFePO_4$ with large particle size.

By plugging the AE measured by GITT into mixed control model, we simulated the discharge curves in GITT and obtained lithium ion diffusivity in α (D^{α}_{Li+}) and β (D^{β}_{Li+}) phase and interface mobility (M) during phase transformation for $Li_4Ti_5O_{12}$ and $LiFePO_4$ respectively. For $LiFePO_4$: $D^{\alpha}_{Li+}\sim10^{-14}$-$10^{-13}cm^2/s$, $D^{\beta}_{Li+}\sim10^{-15}$-$10^{-14}cm^2/s$ and $M\sim10^{-15}$mmol/Js; for $Li_4Ti_5O_{12}$: $D^{\alpha}_{Li+}\sim10^{-11}$-$10^{-10}cm^2/s$, $D^{\beta}_{Li+}\sim10^{-12}$-$10^{-11}cm^2/s$ and $M\sim10^{-13}$mmol/Js. The values of D^{α}_{Li+} and D^{β}_{Li+} calculated by mixed control theory were consistent with those gained in one phase region according to traditional GITT and potentiostatic intermittent titration (PITT) method. We also discovered the effects of phase transformation on cyclic voltammetry (CV), and electrochemical impedance spectroscopy (EIS) tests.

14. SUBJECT TERMS
Phase transformation; accommodation energy; diffusion coefficient; interface mobility; galvanostatic intermittent titration (GITT);potentiostatic intermittent titration (PITT); cyclic voltammetry (CV), and electrochemical impedance spectroscopy (EIS)

15. NUMBER OF PAGES
17 pages

16. PRICE CODE

17. SECURITY CLASSIFICATION OR REPORT **UNCLASSIFIED**	18. SECURITY CLASSIFICATION ON THIS PAGE **UNCLASSIFIED**	19. SECURITY CLASSIFICATION OF ABSTRACT **UNCLASSIFIED**	20. LIMITATION OF ABSTRACT **UL**

Enclosure 1

STIR---Novel Electro-analytical Tools for Phase-Transformation Electrode Materials

Grant # W911NF0810441

September 01, 2008 to June 01, 2009

Submitted by:

Chunsheng Wang, Ph.D.
Principal Investigator
Department of Chemical and Biomolecular Engineering
University of Maryland
College Park, Maryland 20740
Phone: 301-405-0352
cswang@umd.edu

Table of Contents

Appendixes

Final Progress Reports

1. Objective

The objectives of this project are to develop novel electrochemical techniques and to discover structure-phase transformation-electrochemical performance relationships of phase transformation electrodes by using of novel electrochemical techniques.

2. Approach

- To develop novel electrochemical techniques by integrating mixed control theory into traditional electrochemical techniques, such as galvanostatic intermittent titration (GITT), potentiostatic intermittent titration (PITT), cyclic voltammetry (CV), and electrochemical impedance spectroscopy (EIS) (Fig. 1)
- To accurately determine diffusion coefficient and interface mobility of phase transformation materials using novel electrochemical techniques
- To discover the relationships among structure, phase transformation and electrochemical performance by using novel electrochemical techniques.
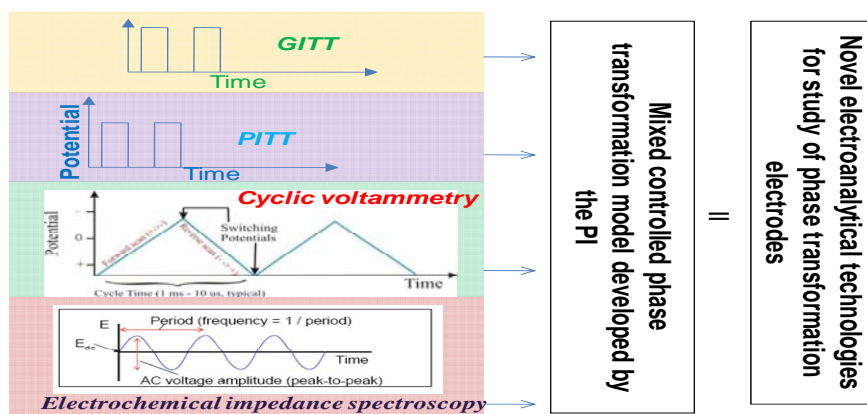

Figure 1 Novel electroanalytical technology for phase transformation electrodes according to mixed control theory

3. Relevance to Army

- Lithium ion batteries are primary candidate power sources to meet the military requirements of 'digitization' of the battlefield and 'Silent Watch' operation because of their silent and high energy density characteristics.
- Rechargeable Li-ion batteries with high power and energy density can be developed based on the knowledge gained from this project, which will extend the mission of solders.
- These research activities in high power electrode materials and analytical techniques would help U.S. stay in a lead position in these strategic fields

4. Accomplishments for Reporting Period

4.1 Electrode and cell preparation

$Li_4Ti_5O_{12}$ and $LiFePO_4$ (nano and micro size) electrodes were prepared using slurry coating method. $Li_4Ti_5O_{12}$ particles were supplied by Ishihara Sangyo Kaisha, Japan. Particle size is between 80 and 200 nm (Fig. 2). Both nano (200~800nm) (Fig. 2) and micro (2~10 μm) (Fig. 2) size $LiFePO_4$ were supplied by an industry, USA. Both $Li_4Ti_5O_{12}$ and $LiFePO_4$ active materials were mixed with 10wt% carbon black and 8wt% Polyvinylidene Fluoride (PVDF) in 1-methyl-2-pyrrolidinone (NMP) solvent to form viscous paste, which was then mixed by ball milling over night. The paste obtained then was coated on carbon coated aluminum foil for $LiFePO_4$ and on carbon coated copper foil for $Li_4Ti_5O_{12}$. The foil then was dried in a vacuum oven at 120 °C overnight. After the foil cooled down to room temperature, electrodes with area $1.26cm^2$ (cut by circular blade with ½ inch diameter, for coil cells) and 2×2 cm^2 (for 3-electrode pouch cells) were cut out with active materials loading between $2mg/cm^2$ and $5mg/cm^2$. Both coil cells and 3-electrode pouch cells for $Li_4Ti_5O_{12}$ and $LiFePO_4$ (nano and micro size) were prepared for electrochemical testing (App.A). All the cells were assembled in an argon-filled glove box, with lithium foil as anode, 1.0M $LiPF_6$ in EC-DEC-DMC-EMC (1:1:1:1:3 by volume) (Ferro Corporation) as liquid electrolyte, and polypropylene (PP) microporous film as separators. Galvanostatic intermittent titration (GITT) and potentiastatic intermittent titration (PITT) tests were performed on Arbin instrumentation. Both cyclic voltammetry (CV) and electrochemical impedance spectroscopy (EIS) tests were preceded on Solartron.
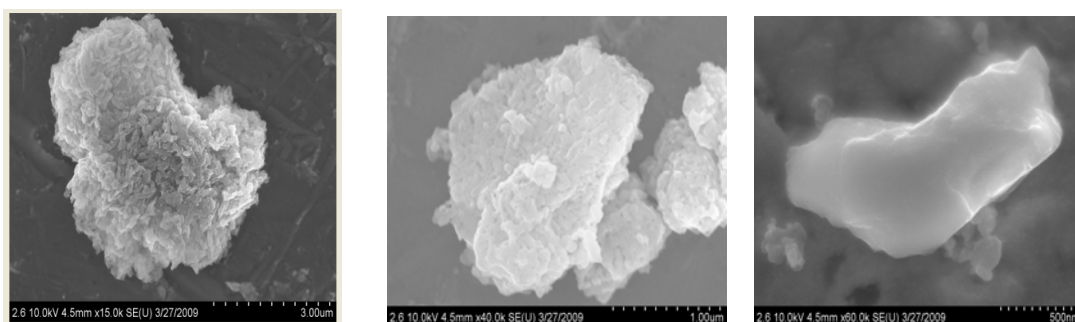

Figure 2 Scanning electron micrograph for testing materials, from left to right, $Li_4Ti_5O_{12}$, accumulated nano sized $LiFePO_4$ and micro sized $LiFePO_4$

4.2 *Determination of accommodation energy for LiFePO₄ and Li₄Ti₅O₁₂*

The strain and stress will be generated during lithium ions insertion into and extraction from phase transformatin materials due to the volume difference between two phases in the materials. The strain and stress creat an elastic and/or plastic accommodation energy, which can be measured by GITT. Figure 3 illustrated the potential response during charge/discharge GITT. Figure 4 showed the accommodation energy changes during phase transformation which was calculated by multiplying Faraday's constant with the potential difference ($\delta V_{\alpha\rightarrow\beta}$, $\delta V_{\beta\rightarrow\alpha}$) between the real equilibrium potential and strain/stress-free equilibrium potential.

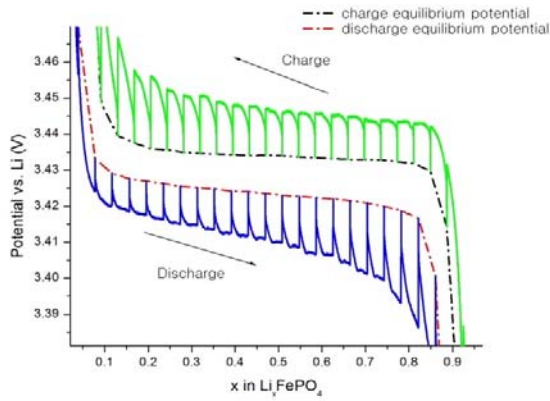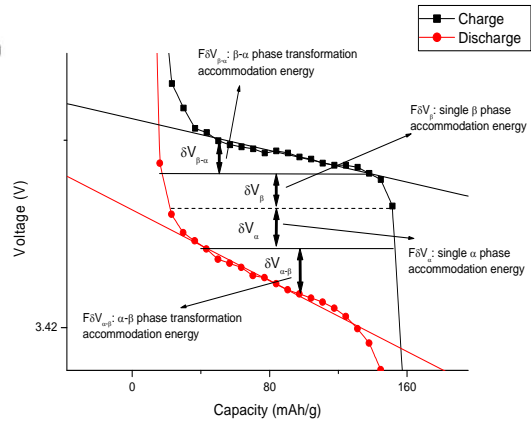| Figure 3 GITT curves of LiFePO₄ with micro size	Figure 4 Determination of accommodation energy for phase transformation materials

a. Accommdation energy difference between charge and discharge

Figure 5 showed that the difference between charge and discharge accommodation energy in the first and second charge/discharge cycles. Obviously, discharge accommodation energy is larger than charge, which can explain why charge is faster than discharge under same rate. The better performance of LiFePO₄ in the charge than that in the dischrge has been reported by several researchers. It was attributed only to the higher diffusion coefficient in the charge than in the discharge which is difficult to be justfied. Our results demonstrated that accomodation energy is resposible for the better charge performance.
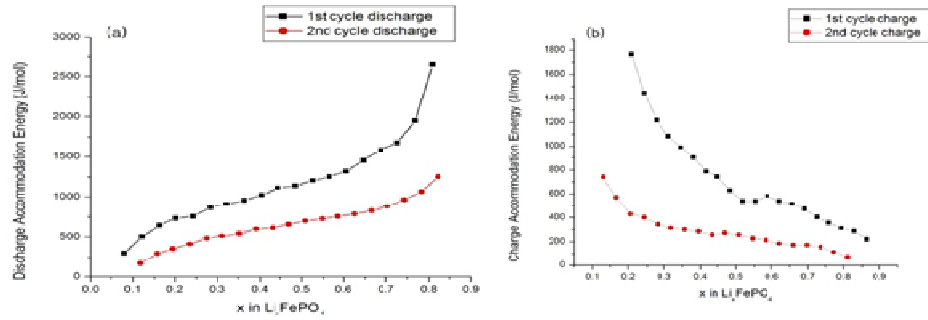
5

Figure 5 Accommodation energy changes of micro-LiFePO$_4$ during 1st and 2nd discharge (a) and charge (b) cycles

b. Accommodation energy changes with charge/discharge cycles

As showed in Figure 5 , the accommodation energies for charge and discharge in first cycle are larger than second cycle. This is due to the activation process (introducing defects) in the first cycle, which did not exist in next cycles.

c. Effect of LiFePO$_4$ particle size on the accommodation energy and electrode performance

Figure 6 showed the accommodation energy for nano and micro sized LiFePO$_4$ particles. As showed in the figure, charge and discharge accommodation energy in nano sized LiFePO$_4$ is lower than that in micro sized LiFePO$_4$. The reduced accommodation energy in nano-LiFePO$_4$ can be attributed to the small miscibility gap in nano-size LiFePO$_4$. The reduced miscibility gap will form a coherent interface resulting in a low plastic accomodation energy.
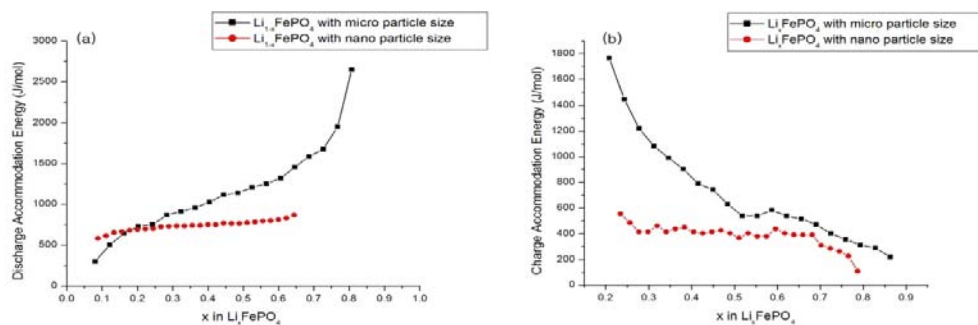

Figure 6. Accommodation energy of LiFePO$_4$ with different particle size during (a) discharge and (b) charge

d. Accommodation energy for different materials

6

Figure 7 showed charge and discharge accommodation energy for $Li_4Ti_5O_{12}$ and $LiFePO_4$. The accommodation energy for $Li_4Ti_5O_{12}$ is much lower than that in $LiFePO_4$. The reason for this is that the two phases volume difference in $Li_4Ti_5O_{12}$ is much smaller comparing to that in $LiFePO_4$.
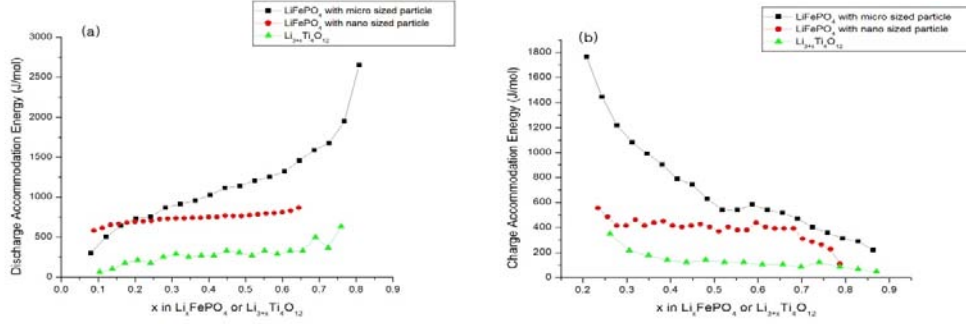

Figure 7 Discharge and charge accommodation energy for $LiFePO_4$ and $Li_4Ti_5O_{12}$ (a) discharge accommodation energy (b) charge accommodation energy

e. Discharge path dependance of charge accomodation energy at different state of charge (SOC)

As showed in Figure 8 , we discharged two $LiFePO_4$ cells (nano and micro particle size) to different state of discharge (SOD) and then charged the cells back to certain point (voltage reached 4.2V) both using GITT. As showed in Figure 8 (a) and (c), the charge equilibrium potentials are different to each other under same SOC, which means the charge accommodation energy might be history dependent. To discover intrinsic principle of this phenomena, we differentiated the GITT charge equilibrium potential with lithium content x in Li_xFePO_4 for different SOD and found that the slopes of them were same. So, at the same SOC, the difference in charge equilibrium potentials was because they had different starting SOD. We also could conclude from above that at different SODs, if we charge them to the same capacity, the net increased in accommodation energy would be the same.
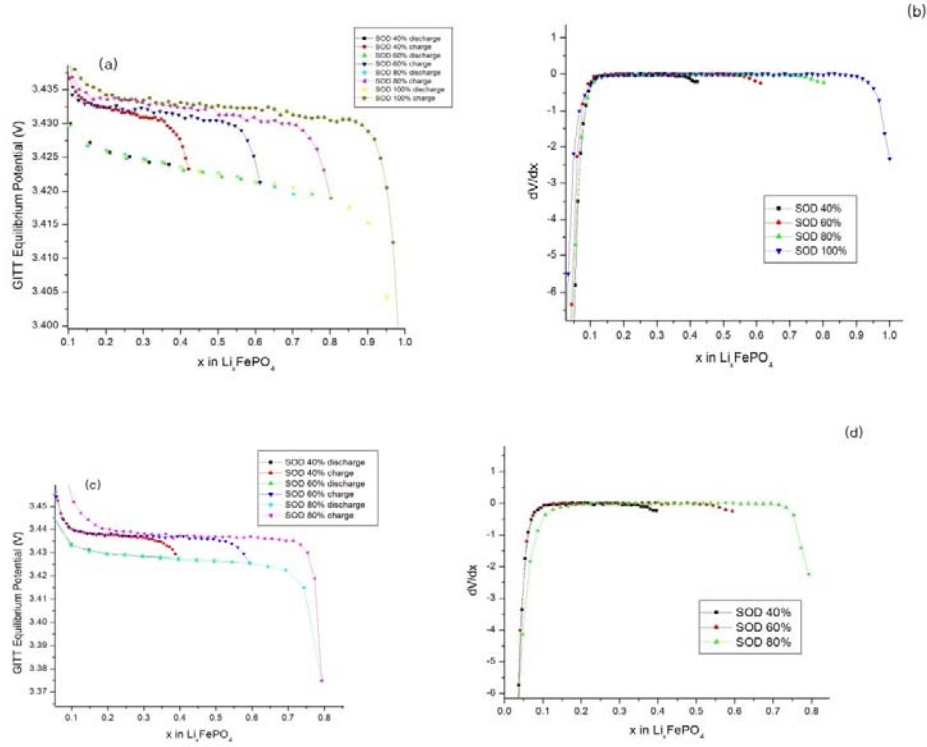
7

Figure 8 Charge equilibrium potential and corresponding potential differential (b and d) of LiFePO$_4$ with macro-size (a) and nano-size (c) after discharging to the different states

f. Accommodation energy determined by cyclic voltammetry (CV)

Another approach to determine the accommodation energy is the CV. The average hysteresis for phase transformation electrodes can be determined by extending the both the charge and discharge current lines to the potential axis. The potential difference is the equilibrium potential hysteresis. Figure 9 demonstrated that the hysteresis (14 mV in Fig.9b) of micro-LiFePO$_4$ measured using CV is almost the same the value (13 mV in Fig. 9c) determined using as GITT. Similarly, the average potential hystersis (4mV in Fig. 9 e) of Li$_4$Ti$_5$O$_{12}$ determined using CV has the same value (4 mV in Fig. 9f) determined using GITT at 50% SOD.

8
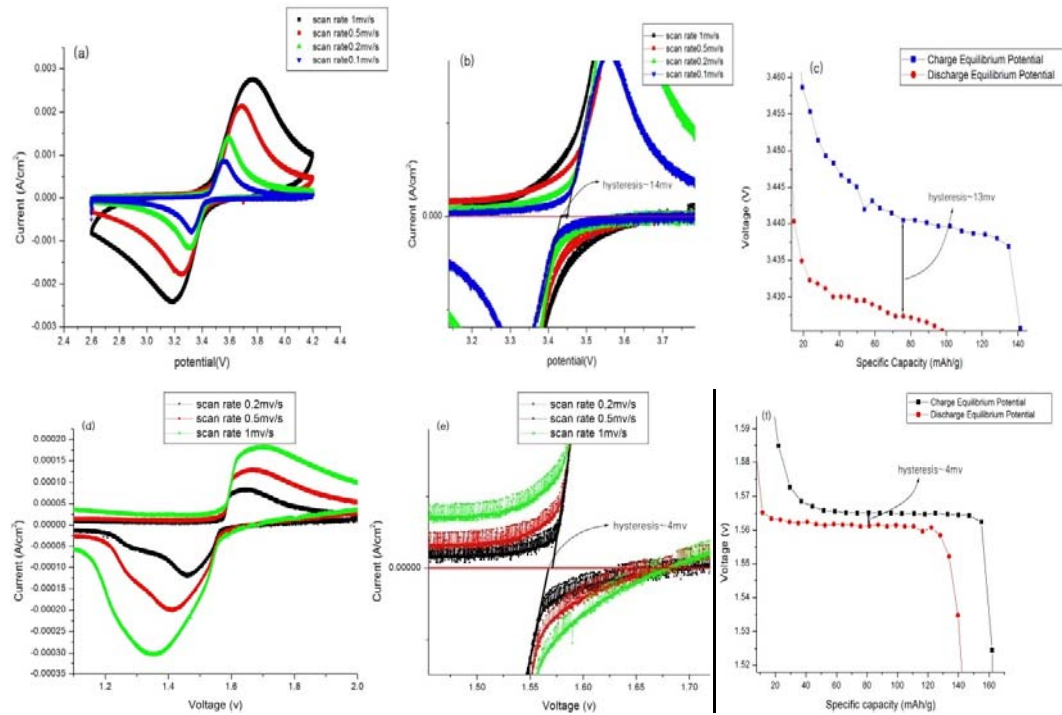
Figure 9 (a) CV scan for LiFePO₄ with micro particle size (b) hysteresis determination in CV for LiFePO₄ (c) hysteresis in GITT for LiFePO₄. (d) CV scan for Li₄Ti₅O₁₂ (e) hysteresis determination in CV for Li₄Ti₅O₁₂ (f) hysteresis in GITT for Li₄Ti₅O₁₂

g. Effects of accommodation energy on cell performance

   To discover the effect of accommodation energy on cells' performance, we tested two LiFePO₄ cells (nano and micro particle size) with different discharge rates. The result was illustrated in Figure 10. From Figure 10, we can obtain that at same discharge rate, LiFePO₄ with nano particle size had higher rate capability, which is attributed to the lower accommodation energy.
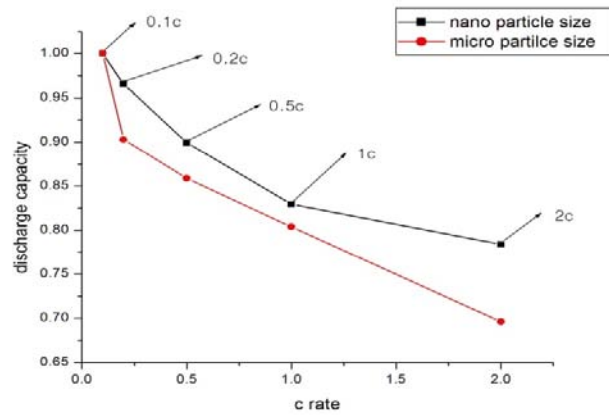

Figure 10 Discharge rate capability for LiFePO₄ with different particle sizes

9

4.3 Determination of diffusion coefficients and interface mobilities by galvanostatic intermittent titration (GITT).

In GITT experiments, we discharged/charged the cell for 1 hour and followed by 16 hours rest. This process will be repeated until the cell voltage reached the upper or low limits (2.2v and 4.2v, separately). The discharge and charge accommodation energy was plugged in our mixed control model to simulate the diffusion coefficient and interface mobility through fitting the simulated value with experimental GITT data.

a. Diffusion coefficients and interface mobilities for nano sized $LiFePO_4$ particle

Figure11 compared the experimental voltage response in a discharge GITT at different state of discharge and simulated values using mixed control theory. The experiment results agreed well with the simulation ones in Figure 11, which validated our mixed control model.
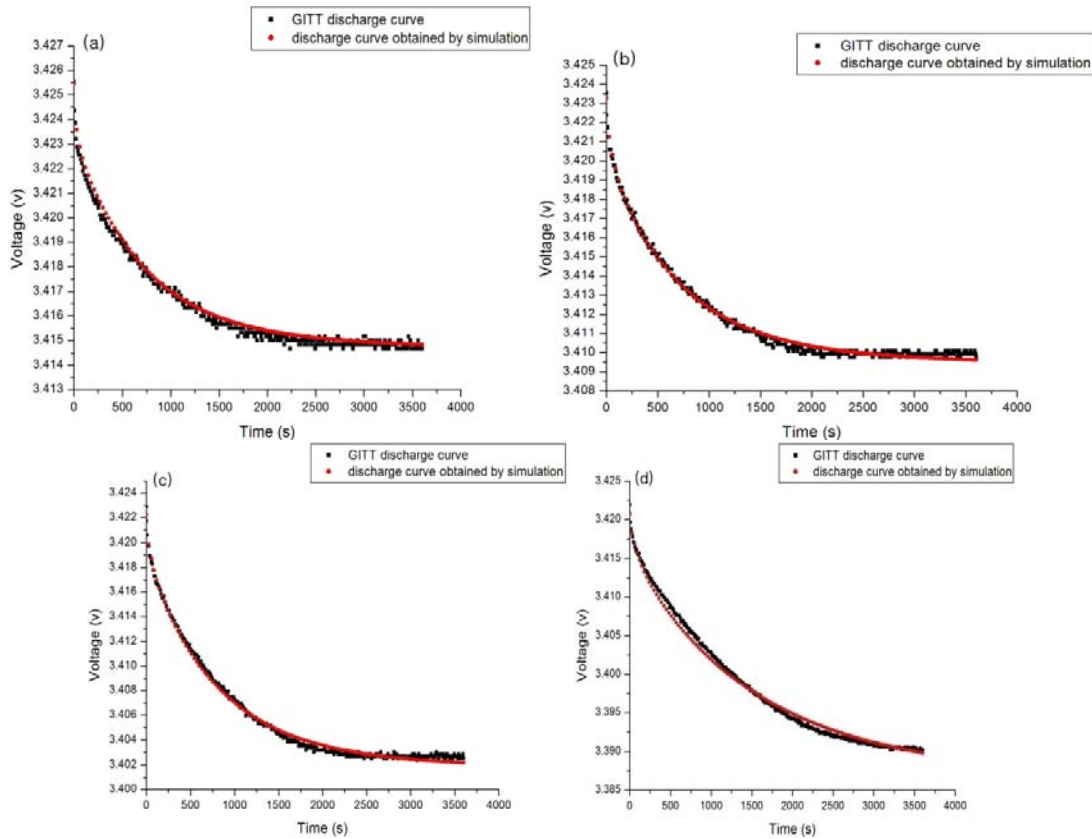

Figure 11 discharge curves of nano-$LiFePO_4$ obtained by GITT and simulation for different SOD (a) 20% (b) 40% (c) 60% (d) 80%

We also calculated the diffusion coefficient of nano-LiFePO$_4$ using the traditional GITT method and compared it with mixed control theory in Figure 12, where D$^\beta_{Li+}$ and D$^\alpha_{Li+}$ mean lithium ion diffusivity in α and β phase separately.
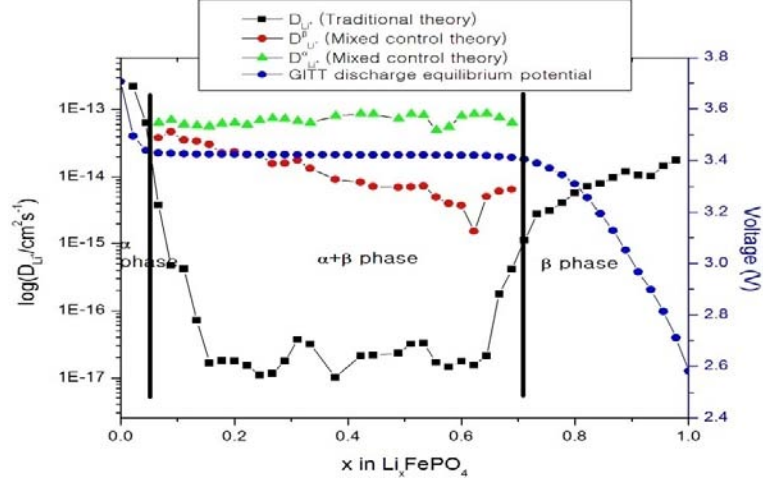

Figure 12 Lithium ion diffusion coefficients calculated by traditional and mixed control theory for nano sized LiFePO$_4$

Since traditional GITT theory was developed based on solid solution model, it is precise only in one phase region (pure α or β only). If we applied traditional GITT in two phase region, we only can get one diffusion coefficient, which is called "apparent diffusion coefficient" and whose values are lower 2~3 orders than those in one phase region as shown in Figure 12 (black square marks). By applying mixed control theory, we can obtain lithium ion diffusivity in α and β phases individually and the values are almost the same order as those in one phase reigon and reported by other authers [1],[2].

We also obtained the interface mobility during the discharge process (Figure 13), which is unable to be calculated in traditional GITT. The interface mobility values were around 10^{-15} mmol/Js order.
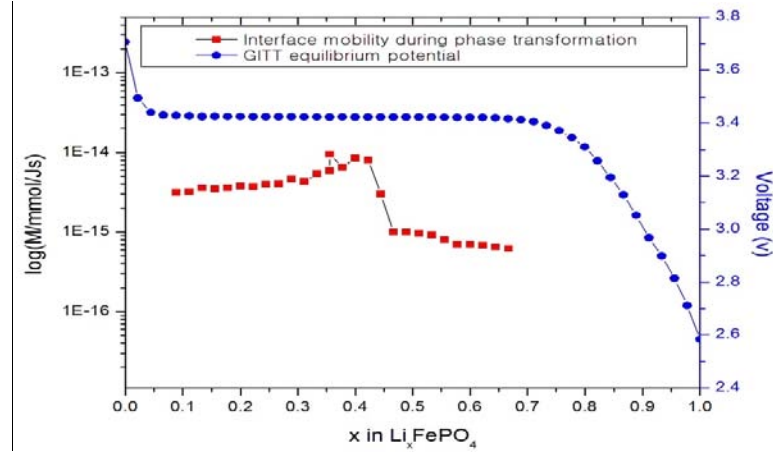
11

Figure 13 Interface mobility values for nano sized LiFePO$_4$ during GITT discharge

b. Diffusion coefficients and interface mobilties for Li$_4$Ti$_5$O$_{12}$ particle

We also calculated the lithium ions diffusivity for Li$_4$Ti$_5$O$_{12}$ in Figure 14. As shown in Figure 14, same results obtained as for LiFePO$_4$, the diffusion coefficient values obtained according to traditional GITT were 2~3 orders lower than those in single phase region, which is unreasonable. The values calculated by mixed control theory were close to those in one phase region, but 5~7 times higher. We attrbuted this small difference to the unprecise accommodation energy we measured. The reported voltage difference between the beginning and the ending of phase transformation is less than 3mv for
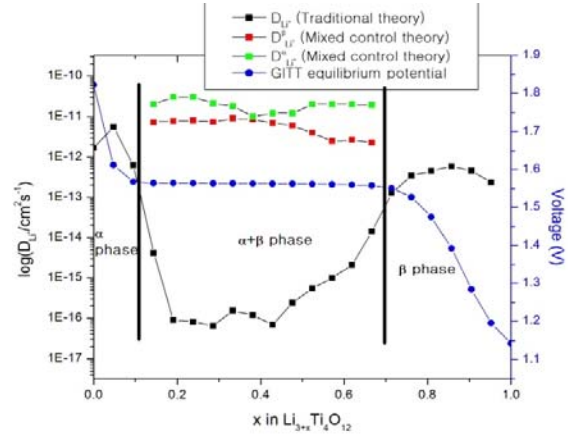

Figure 14 Lithium ion diffusivity calculated by traditional and mixed control theory

GITT equilibrium potential during discharge. The potential differnce we measured was around 7mv, which is due to the insufficient rest time (16 hours in this case) for GITT test. Since we overestimated the discharge accommodation energy, the resulted diffusion coefficient was higer than that in one phase region.

12

We also obtained the interface mobilty for $Li_4Ti_5O_{12}$ during discharge GITT in Fugure 15. The values were around 10^{-13} mmol/Js order, which is almost 100 times higher than that for $LiFePO_4$.
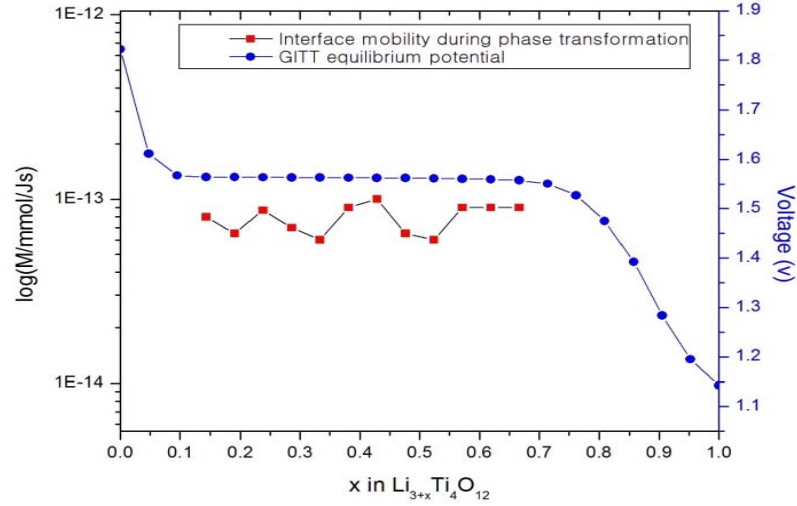

Figure 15 Interface mobility values for $Li_4Ti_5O_{12}$ during GITT discharge

4.4 Determination of diffusion coefficients and interface mobilities by potentiostatic intermittent titration (PITT)

To cross check the validity of mixed control theory, we also performed PITT tests on $LiFePO_4$ and $Li_4Ti_5O_{12}$ cells and calculated lithium ion diffusivity.

a. Diffusion coefficients of nano sized $LiFePO_4$

   The lithium diffusivity in nano sized $LiFePO_4$ was calculated using traditional PITT and was shown in Figure 16. The diffusion coefficient values well agreed with those calculated by GITT in single phase. In two phase region, the diffusivity is lower about 3~4 times than that in one phase region due to the pre-assumption (single phase only) of traditional PITT method .
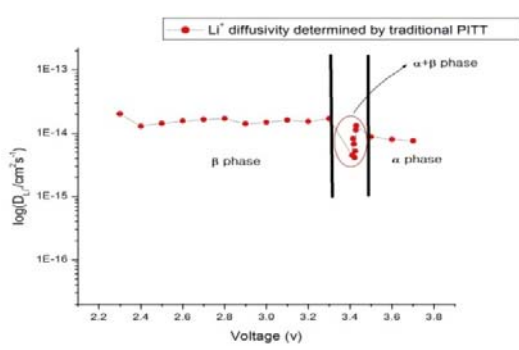
b. Diffusion coefficients for $Li_4Ti_5O_{12}$

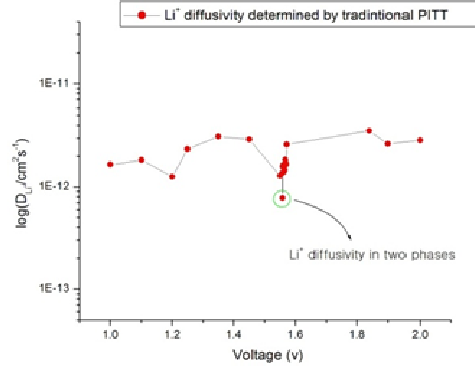| Figure 16 Diffusion coefficient calculated by traditional PITT method for nano sized LiFePO$_4$	Figure 17 Diffusion coefficient calculated by traditional PITT method for Li$_4$Ti$_5$O$_{12}$

We also calculated lithium ion diffusion coefficient in Li$_4$Ti$_5$O$_{12}$ using traditional PITT method in Figure 17.

The results in single phase obtained by traditional PITT were close to those in traditional GITT and measured by other authers [3]. Due to the narrow voltage range of two phase region in Li$_4$Ti$_5$O$_{12}$, there was only one diffusivity in two phase region. The diffusion coefficient in two pgase region is lower than that in a single phase region.
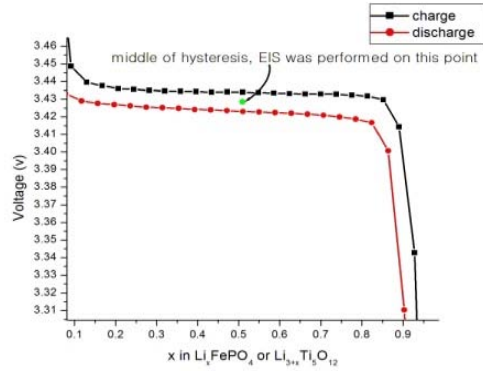
Since the voltage range of two phase region is pretty narrow (LiFePO$_4$~10mv, Li$_4$Ti$_5$O$_{12}$~2mv), it is not easy to perform PITT tests only in two phases region if the resolution of testing machine is low. There are only few points in two phases region (for Li$_4$Ti$_5$O$_{12}$, only one point). However we used PITT results in single phase to cross check GITT results and mixed control theory. The similarity between the diffusion coefficient in the single phase region and that in two phase region validitied our mixed control model.

4.5 Determination of diffusion coefficients and interface mobilities by electrochemical impedance spectroscopy (EIS)

Traditional EIS was also based on pure solid solution condition. To probe the effect of phase transformation on EIS, we first discharged the cell to 50% SOD, then charged it back to the middle of hysteresis and performed EIS on the point, which was demonstrated on Figure 18. At this point, we performed EIS with different

amplitudes (frequency from 10^6 to 0.001 Hz). The results were showed in Figure 19. If amplitude EIS is lower than half of voltage hysteresis in GITT (For LiFePO$_4$ is ~7mv, Li$_4$Ti$_5$O$_{12}$ ~1.5mv), the values of real and imagine part of

Figure 18 Illustration of starting point for EIS

of

impedance were almost the same. But once the EIS amplitude is larger than half of voltage hysteresis, the values for real and imagine parts decreased significantly. We attributed this phenomena to the new phase formed when the EIS amplitude was larger than half of voltage hysteresis. To prove this mechanism, we simulated the EIS according to above physical process. Also we had to notice that even when the EIS amplitude was lower that half of voltage hysteresis, the traditional EIS theory is still need to be modified although there is no phase transformation in this region. This is because the material contained two phases which is different with the assumption made by traditional EIS.
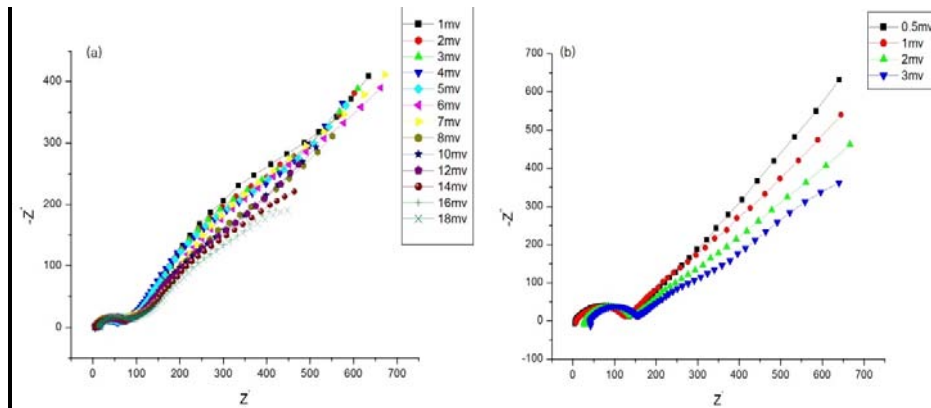

Figure 19 EIS with different amplitudes (a) for LiFePO$_4$ (b) Li$_4$Ti$_5$O$_{12}$

4.6 Determination of diffusion coefficients and interface mobilities by cyclic voltammetry (CV)

To develop novel CV and discover the intrinsic mechanism of phase transformation, we performed CV tests at different initial states and different voltage ranges. Figure 9 showed the results for CV tests over both single and two phase

regions. The hysteresis in CV agreed well with that in GITT. We also measured CV at SOC 50% for LiFePO$_4$ in Figure 20. In Figure 20, we performed CV on SOC 50%, starting from open circuit voltage (OCV) of SOC 50%, scanning voltage down to some value lower than OCV of SOC 50%, and then back to OCV. As shown in Figure 20, if the scan voltage range was larger than phase transformation voltage hysteresis (~14mv), the current vs. voltage plot changed significantly due to the formation of new phase. Same phenomena also happened when we performed CV on SOD 50% in Figure 21. Currently we are repeating this physical process and getting the diffusivity and interface mobility for phase transformation by simulation according to mixed control theory.
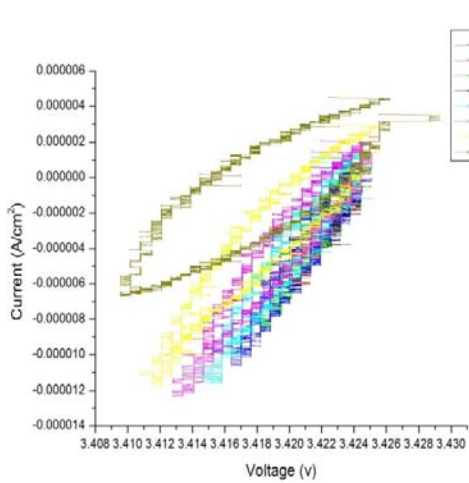

Figure 20 CV on SOC 50% for LiFePO$_4$

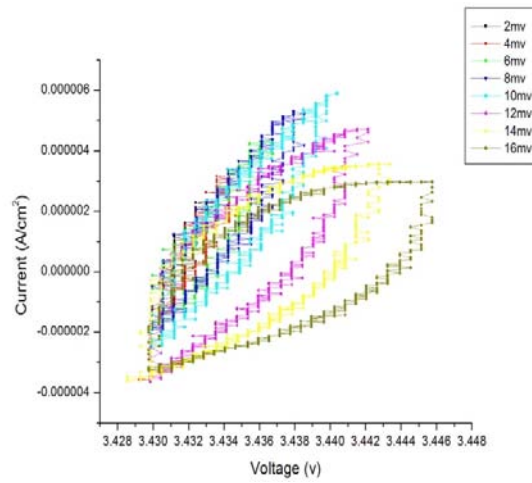Figure 21 CV on SOD 50% for LiFePO$_4$

5. Future work for this project

To finish and develop this project, we plan to do follow things in the future: first, we will complete and validate the simulations for EIS and CV by using mixed control theory; second, calculate the diffusivity and interface mobility using novel EIS and CV and cross check the results by GITT and PITT; third, investigate relationships among structure, phase transformation, electrochemical performance; fourth, optimize current high power phase transformation electrodes and develop next generation high power electrode materials.

References

[1] P. P. Prosini, M. Lisi, D. Zane,M. Pasquali, Solid State Ionics. 148 (2002) 45-51

[2] J. Xie, N. Imanishi, T. Zhang, A. Hirano, Y. Takeda, O. Yamamoto, Electrochimica Acta. 54 (2009) 4631-4637

[3] Y. H. Rho, K. Kanamura, J. Solid State Chem 177 (2004) 2094-2100

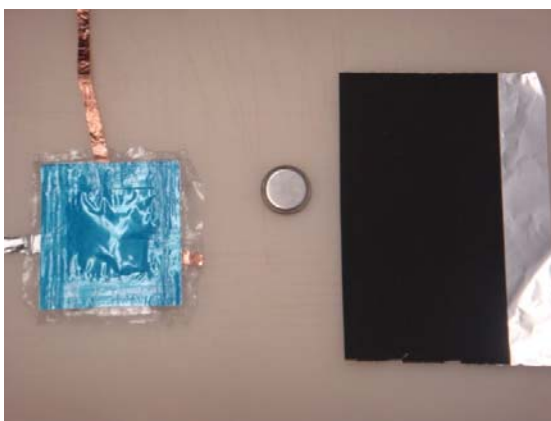**Appendixes**

   A. Electrodes and cells used in tests

Figure 22 From left to right, three-electrode pouch cell, two-electrode coin cell, and LiFePO$_4$ cathode.